



Open Research Online

The Open University's repository of research publications and other research outputs

Rotation symmetry axes and the quality index in a 3D octahedral parallel robot manipulator system

Book Section

How to cite:

Tanev, T. K. and Rooney, J. (2002). Rotation symmetry axes and the quality index in a 3D octahedral parallel robot manipulator system. In: Lenarcic, Jadran and Thomas, Federico eds. Advances in robot kinematics: theory and applications. Kluwer Academic Publishers, pp. 29–38.

For guidance on citations see [FAQs](#).

© [not recorded]

Version: [not recorded]

Link(s) to article on publisher's website:

<http://www.springer.com/uk/home?SGWID=3-102-22-33703447-0&changeHeader=true>

Copyright and Moral Rights for the articles on this site are retained by the individual authors and/or other copyright owners. For more information on Open Research Online's data [policy](#) on reuse of materials please consult the policies page.

oro.open.ac.uk

ROTATION SYMMETRY AXES AND THE QUALITY INDEX IN A 3D OCTAHEDRAL PARALLEL ROBOT MANIPULATOR SYSTEM

T. K. Tanev and J. Rooney
Department of Design and Innovation
The Open University, UK
t.k.tanev@open.ac.uk
j.rooney@open.ac.uk

Abstract The geometry of a 3D octahedral parallel robot manipulator system is specified in terms of two rigid octahedral structures (the fixed and moving platforms) and six actuation legs. The symmetry of the system is exploited to determine the behaviour of (a new version of) the quality index for various motions. The main results are presented graphically.

Keywords: parallel robot, quality index, rotation symmetry

1. Introduction

In recent years there has been much interest in the geometry of the Stewart platform (Stewart, 1965) and this work has led to the development of various parallel manipulation systems. Several kinematic performance indices have been introduced (Yoshikawa, 1985, Angeles and Lopez-Cajun, 1992, Lee, Duffy and Hunt, 1998, Lee, Duffy and Keler, 1999). In particular the so-called quality index (Lee, Duffy and Hunt, 1998, Lee, Duffy and Keler, 1999) has been used widely. The values of the index are usually plotted for a range of movements of the platform within the workspace. Investigators have usually defined the quality index as the ratio of the *absolute* value of the Jacobian determinant to the *maximal absolute* value of the Jacobian determinant. Hence because of the use of absolute values, the usual quality index lies in the range (0,1). Moreover, symmetry arguments have often been used to restrict examination of the behaviour of the quality index to configurations for which the manipulator is close to its central 'home' position.

In this paper, we investigate a system generalized from the Stewart platform in two ways. Firstly, we generalize the geometry of the manipulator to produce a system consisting of a *3D-solid* moving platform and a *3D-solid* fixed platform (so that neither the six joints on the moving platform nor those on the fixed platform lie in single

planes). Secondly, we introduce a new form of the quality index, which does not involve absolute values. We calculate and plot the actual values (positive, zero and negative) of this new quality index for a *two*-parameter family of movements (either a one-parameter family of rotations about a one-parameter family of rotation axes, or a two-parameter family of screw motions about a single fixed screw axis). The plot yields a surface since two parameters are varied. The paper presents an exploration of the type of behaviour possible in highly symmetrical parallel systems more general than the Stewart platform. Further work is planned to extend the approach to systems with progressively less symmetry. Systems whose geometry differs only slightly from the highly symmetrical case presented here become asymmetrical, yet they retain very similar general characteristics in the behaviour of the quality index.

2. Geometry and Symmetry of 3D Octahedral 6-6 Platforms

The geometry of the Stewart parallel manipulator (Stewart, 1965) is octahedral in the sense that, in a typical position, the moving triangular platform and the fixed triangular base form opposite faces of an octahedron, and the six legs form the edges of the other six triangular faces (Fig. 1) (Lee, Duffy and Hunt, 1998). Often the dimensions are such that the moving and fixed platforms are congruent equilateral triangles and in the 'home' position each of the six legs has the same length, equal to the length of the platform edge. In this position the system forms a regular octahedron, but in most other positions the polyhedral regularity is lost and the system has the geometry of a scalene octahedron. However, since the triangular platforms are rigid they remain regular polygons throughout any motion. Both the moving platform and the fixed platform have an axis of 3-fold rotation symmetry, together with three planes of reflection symmetry perpendicular to the platform surface.

It is possible to generalize the Stewart platform geometry by re-locating the spherical joints in a 2D polygonal arrangement other than an equilateral triangle (see for example Duffy, Rooney, Knight and Crane, 2000, Merlet, 1993, Mayer St-Onge and Gosselin, 2000, Zanganeh and Angeles, 1997). In general this will form a (non-regular) hexagon (Fig.1). The resulting system still consists of an hexagonal platform moving with respect to a fixed hexagonal platform. Similar generalizations lead to quadrilateral, pentagonal and in general planar polygonal platforms [Rooney, Duffy and Lee, 1999].

However, a 3D arrangement of the spherical joints is possible. A particular example of this further generalization is shown in Fig.1 where the joints on the moving 'platform' are located at the vertices of a regular solid octahedron. The joints on the fixed platform may be similarly arranged at the vertices of a different regular solid octahedron and the resulting system then has a more general geometry than previous types of parallel robot manipulator derived from the Stewart platform.

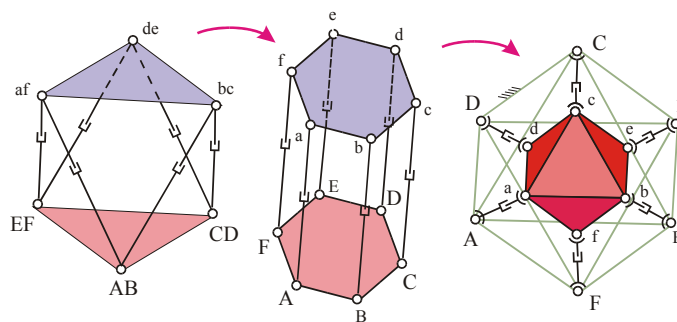


Figure 1. Three types of 6-6 parallel manipulator, progressively more general.

The moving 'platform' now itself has the shape, and hence the symmetry, of a regular octahedron (Fig.2).

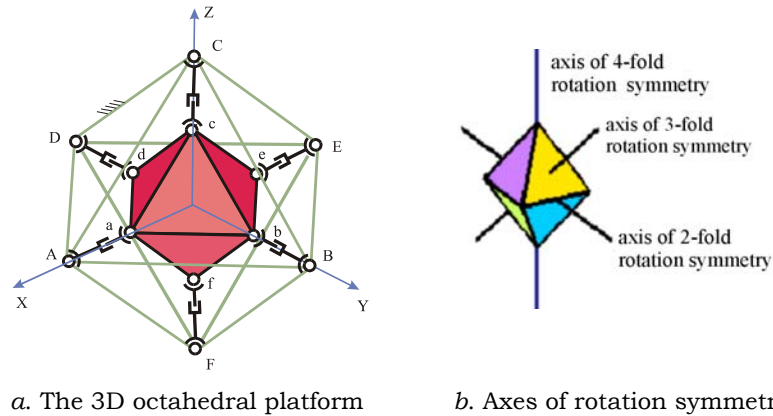


Figure 2. The 3D octahedral platform and some axes of rotation symmetry

The latter has three 4-fold axes of rotation symmetry (each passing through a pair of opposite vertices), four 3-fold axes of rotation symmetry (each passing through the centers of a pair of opposite

faces), and six 2-fold axes of rotation symmetry (each passing through the centers of a pair of opposite edges). There are also several types of planes of reflection symmetry, one of which passes through two opposite vertices and bisects the solid octahedron. This generalized parallel manipulator system is referred to as a 3D octahedral platform.

3. The 3D Octahedral Platform and its Quality Index

The octahedral manipulator shown in Fig. 2 is fully parallel and it has a linear actuator on each of its six legs. The six spherical joints of the moving platform are situated at the vertices of a regular octahedron and similarly the six spherical joints of the base are situated at the vertices of another regular octahedron. These two octahedra are each dual to a cube. It is well known that the cube and the octahedron are dual to each other. The first octahedron is formed by joining the centers of adjacent faces of the cube. The size of the second one is chosen in a way that the edge of the octahedron is perpendicular to its parent (the edge of the cube) and cuts through the parent at its midpoint (Fig. 3).

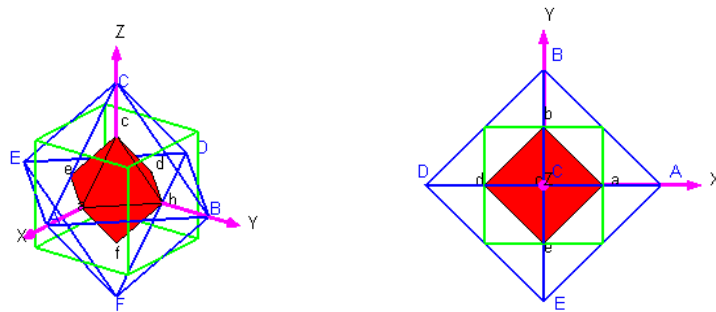


Figure 3. 3D representation and a plan view of the two octahedra and the dual cube.

Let σ denote the edge length of the outer octahedron, then the coordinates of the edges of the octahedrons are [Lee, Duffy and Rooney, 2000]:

$$\begin{aligned} A: & \begin{bmatrix} \frac{\sigma}{\sqrt{2}} & 0 & 0 \end{bmatrix}, B: \begin{bmatrix} 0 & \frac{\sigma}{\sqrt{2}} & 0 \end{bmatrix}, C: \begin{bmatrix} 0 & 0 & \frac{\sigma}{\sqrt{2}} \end{bmatrix}, \\ D: & \begin{bmatrix} -\frac{\sigma}{\sqrt{2}} & 0 & 0 \end{bmatrix}, E: \begin{bmatrix} 0 & -\frac{\sigma}{\sqrt{2}} & 0 \end{bmatrix}, F: \begin{bmatrix} 0 & 0 & -\frac{\sigma}{\sqrt{2}} \end{bmatrix} \end{aligned} \quad (1)$$

$$\begin{aligned}
a: & \begin{bmatrix} \frac{\sigma}{2\sqrt{2}} & 0 & 0 \end{bmatrix}, \quad b: \begin{bmatrix} 0 & \frac{\sigma}{2\sqrt{2}} & 0 \end{bmatrix}, \quad c: \begin{bmatrix} 0 & 0 & \frac{\sigma}{2\sqrt{2}} \end{bmatrix}, \\
d: & \begin{bmatrix} -\frac{\sigma}{2\sqrt{2}} & 0 & 0 \end{bmatrix}, \quad e: \begin{bmatrix} 0 & -\frac{\sigma}{2\sqrt{2}} & 0 \end{bmatrix}, \quad f: \begin{bmatrix} 0 & 0 & -\frac{\sigma}{2\sqrt{2}} \end{bmatrix}
\end{aligned} \tag{2}$$

The origin of the fixed coordinate frame is placed at the center of the outer octahedron and the origin of the coordinate frame attached to the moving platform is at the center of the inner octahedron.

The Plücker line coordinates of the six legs can be expressed by Grassmann determinants. Hence, the direction ratios of the line are

$$L = \begin{vmatrix} 1 & x_1 \\ 1 & x_2 \end{vmatrix}, \quad M = \begin{vmatrix} 1 & y_1 \\ 1 & y_2 \end{vmatrix}, \quad N = \begin{vmatrix} 1 & z_1 \\ 1 & z_2 \end{vmatrix}, \tag{3}$$

and the moments of the line segments about the coordinate axes are

$$P = \begin{vmatrix} y_1 & z_1 \\ y_2 & z_2 \end{vmatrix}, \quad Q = \begin{vmatrix} z_1 & x_1 \\ z_2 & x_2 \end{vmatrix}, \quad R = \begin{vmatrix} x_1 & y_1 \\ x_2 & y_2 \end{vmatrix}, \tag{4}$$

where (x_1, y_1, z_1) and (x_2, y_2, z_2) are coordinates of two point of the line.

Let the position and orientation of the moving octahedron with respect to the fixed octahedron be given by the transformation matrix \mathbf{A} , where

$$\mathbf{A} = \begin{bmatrix} l_1 & l_2 & l_3 & s_x \\ m_1 & m_2 & m_3 & s_y \\ n_1 & n_2 & n_3 & s_z \\ 0 & 0 & 0 & 1 \end{bmatrix} \tag{5}$$

Then using eqs.(3) and (4), the Plücker line coordinates of the six legs (Fig.2) can be written as:

$$\begin{aligned}
s_1 &= \left[\frac{\sqrt{2}}{2} \sigma \left(\frac{l_1}{2} - 1 \right) + s_x, \frac{\sqrt{2}}{4} \sigma m_1 + s_y, \frac{\sqrt{2}}{4} \sigma n_1 + s_z; 0, -\frac{\sqrt{2}}{2} \sigma \left(\frac{\sqrt{2}}{4} \sigma n_1 + s_z \right), \frac{\sqrt{2}}{2} \sigma \left(\frac{\sqrt{2}}{4} \sigma m_1 + s_y \right) \right] \\
s_2 &= \left[\frac{\sqrt{2}}{2} \sigma \left(1 - \frac{l_1}{2} \right) + s_x, -\frac{\sqrt{2}}{4} \sigma m_1 + s_y, -\frac{\sqrt{2}}{4} \sigma n_1 + s_z; 0, \frac{\sqrt{2}}{2} \sigma \left(-\frac{\sqrt{2}}{4} \sigma n_1 + s_z \right), -\frac{\sqrt{2}}{2} \sigma \left(-\frac{\sqrt{2}}{4} \sigma m_1 + s_y \right) \right] \\
s_3 &= \left[\frac{\sqrt{2}}{4} \sigma l_2 + s_x, \frac{\sqrt{2}}{2} \sigma \left(\frac{m_2}{2} - 1 \right) + s_y, \frac{\sqrt{2}}{4} \sigma n_2 + s_z; \frac{\sqrt{2}}{2} \sigma \left(\frac{\sqrt{2}}{4} \sigma n_2 + s_z \right), 0, -\frac{\sqrt{2}}{2} \sigma \left(\frac{\sqrt{2}}{4} \sigma l_2 + s_x \right) \right] \\
s_4 &= \left[-\frac{\sqrt{2}}{4} \sigma l_2 + s_x, \frac{\sqrt{2}}{2} \sigma \left(1 - \frac{m_2}{2} \right) + s_y, -\frac{\sqrt{2}}{4} \sigma n_2 + s_z; -\frac{\sqrt{2}}{2} \sigma \left(-\frac{\sqrt{2}}{4} \sigma n_2 + s_z \right), 0, \frac{\sqrt{2}}{2} \sigma \left(-\frac{\sqrt{2}}{4} \sigma l_2 + s_x \right) \right] \\
s_5 &= \left[\frac{\sqrt{2}}{4} \sigma l_3 + s_x, \frac{\sqrt{2}}{4} \sigma m_3 + s_y, \frac{\sqrt{2}}{2} \sigma \left(\frac{n_3}{2} - 1 \right) + s_z; -\frac{\sqrt{2}}{2} \sigma \left(\frac{\sqrt{2}}{4} \sigma m_3 + s_y \right), \frac{\sqrt{2}}{2} \sigma \left(\frac{\sqrt{2}}{4} \sigma l_3 + s_x \right), 0 \right]
\end{aligned} \tag{6}$$

$$\mathcal{S}_6 = \left[-\frac{\sqrt{2}}{4}\sigma l_3 + s_x, -\frac{\sqrt{2}}{4}\sigma m_3 + s_y, \frac{\sqrt{2}}{2}\sigma \left(1 - \frac{n_3}{2}\right) + s_z, \frac{\sqrt{2}}{2}\sigma \left(-\frac{\sqrt{2}}{4}\sigma m_3 + s_y\right), -\frac{\sqrt{2}}{2}\sigma \left(-\frac{\sqrt{2}}{4}\sigma l_3 + s_x\right), 0 \right]$$

Here, the six leg are as follows (Fig.): $\mathcal{S}_1 = \mathbf{aA}$, $\mathcal{S}_2 = \mathbf{dD}$, $\mathcal{S}_3 = \mathbf{bB}$, $\mathcal{S}_4 = \mathbf{eE}$, $\mathcal{S}_5 = \mathbf{cC}$ and $\mathcal{S}_6 = \mathbf{fF}$.

In this paper the quality index (Lee, Duffy and Hunt, 1998, Lee, Duffy and Keler, 1999) is defined in a new form, without using absolute values, as:

$$\lambda = \frac{\det \mathbf{J}}{|\det \mathbf{J}|_{\max}}, \quad (7)$$

where \mathbf{J} is the 6x6 Jacobian matrix of the normalized coordinates of the six legs.

The normalized Jacobian matrix of the six lines, which are changed to unit length, can then be written as

$$\mathbf{J} = \begin{bmatrix} \frac{1}{l_1}\mathcal{S}_1 & \frac{1}{l_2}\mathcal{S}_2 & \frac{1}{l_3}\mathcal{S}_3 & \frac{1}{l_4}\mathcal{S}_4 & \frac{1}{l_5}\mathcal{S}_5 & \frac{1}{l_6}\mathcal{S}_6 \end{bmatrix} \quad (8)$$

where $l_i = \sqrt{L_i^2 + M_i^2 + N_i^2}$, $i = 1..6$.

The quality index given by eq.(7) takes into account the sign of the determinant of the Jacobian matrix \mathbf{J} , and that is why it is bounded between -1 and 1 , which (depending on the particular configuration) may differ in sign from the quality index defined by Lee, Duffy and Hunt, 1998, and Lee, Duffy and Keler, 1999. A zero value of the quality index indicates singularities and the value 1 (or -1) for the quality index determines the best configuration of the robot. For a particular system the positive orientation on each leg is fixed by convention and hence the value of λ is relative to this convention.

3.1. Extrema of the Jacobian Determinant

In this paper, the quality index is computed with the edge length σ of the outer octahedron equal to 1. Expressing the elements of the matrix \mathbf{A} given by eq.(5) in terms of screw parameters (α, β, ϕ, d) , the determinant of the Jacobian (non-normalized) for screw motions about axes, which pass through the origin of the coordinate system, can be expressed as:

$$\det \mathbf{J}^* = -\frac{\sqrt{2}}{64} \sin(\alpha) \cos(\alpha) \cos(\beta) \sin(\phi) (\cos(\beta)^2 - 1) (5 - 9 \cos(\phi) + 4 \cos(\phi)^2) , \quad (9)$$

where \mathbf{J}^* indicates the non-normalized Jacobian; ϕ is the rotation angle, and α and β are the spherical polar coordinates (longitude and co-latitude) determining the positive direction of the screw axis.

The determinant $\det \mathbf{J}^*$ is equal to zero when: *i*) $\phi = n\pi$ ($n = 0, 1, 2, \dots$); *ii*) $\alpha = n\pi/2$ ($n = 0, 1, 2, \dots$); *iii*) $\beta = n\pi/2$ ($n = 0, 1, 2, \dots$). This implies that the robot is in singular configurations when the screw motion is about the axes of 2-fold and 4-fold rotation symmetry, regardless of the angle of rotation about these axes.

Now, we obtain the maximum value of $\det \mathbf{J}$ the determinant of the normalized Jacobian matrix. We consider rotations about axes that pass through the origin of the coordinate system. In this case, $\det \mathbf{J}$ (not detailed here for lack of space) is a function of three variables,

$$\det \mathbf{J} = f(\alpha, \beta, \phi). \quad (10)$$

Taking the partial derivatives $\partial f / \partial \alpha$, $\partial f / \partial \beta$ and $\partial f / \partial \phi$, and equating to zero yield three equations. We use the tan(half-angle) substitution for $\sin(\phi), \cos(\phi), \sin(\alpha), \cos(\alpha), \sin(\beta),$ and $\cos(\beta)$ in the latter equations. Some of the factors of the above equations lead to the following solutions of the angle $\alpha : \pi/4; -\pi/4; 3\pi/4; -3\pi/4$ (only the solutions which do not yield singular configurations are listed). These angles imply that there is a local maximum of the determinant of the normalized Jacobian matrix for rotations about axes in a plane of reflection symmetry (the axes of rotation of the moving octahedron pass through the origin and lie in a plane of reflection symmetry that passes through two vertices and cuts an edge at its midpoint) (Fig.4a).

Now we consider rotations about axes in a plane of reflection symmetry ($\alpha = \pi/4$). In this case, $\det \mathbf{J}$ is a function of two variables,

$$\det \mathbf{J} = f(\beta, \phi). \quad (11)$$

Again, taking the partial derivatives $\partial f / \partial \beta$ and $\partial f / \partial \phi$, equating to zero and making the tan(half-angle) substitution t_1 for $\sin(\phi), \cos(\phi)$ and t_2 for $\sin(\beta), \cos(\beta)$ yield two equations. Factorising these two equations and solving them together yield the following solutions (only real solutions are listed here): $(t_2 = 0, t_1 = \pm 1.16481293)$, $(t_2 = \pm 1.93185165, t_1 = \pm 0.74267285)$, $(t_2 = \pm 0.51763809, t_1 = \pm 0.74267285)$. Note that two of the factors lead to a polynomial in the single variable (t_2) of order 64. Hence, the resulting angles, that do not yield singular configurations, are: $\beta_{1,2} = \pm 0.95531661$, $\beta_{3,4} = \pm 2.18627603$; $\phi_{1,2} = \pm 1.27759043$. The four solutions for β determine exactly the axes of 3-fold rotation symmetry of the octahedron. This means that the maximum of $\det \mathbf{J}$ occurs for a rotation at $\phi_{1,2} = \pm 1.27759043$ about the axis of 3-fold rotation symmetry.

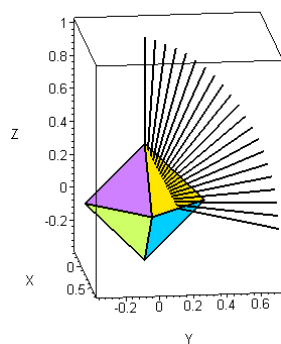
A similar analysis can be carried out for a combined translation and rotation about and along the axis of 3-fold rotation symmetry, which yields the following real solutions for d (the translation

distance) and angle ϕ : $d = 0$; $\phi_{1,2} = \pm 1.27759043$. In this case, two of the factors lead to univariate (t_1) polynomial of order 20. The obtained result implies that the value of the quality index is smaller when translating from the central position.

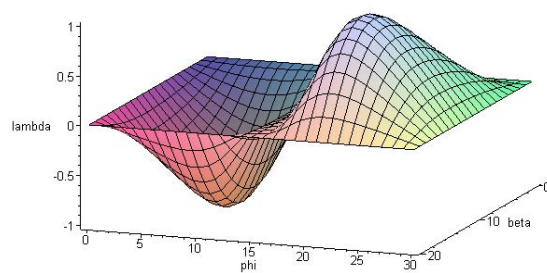
Hence, using the values of the variables obtained above, the maximum absolute value of $\det J$ is obtained as: $|\det J|_{\max} = 0.23455336$.

3.2 Rotation Axes in a Plane of Reflection Symmetry

In this case, the axes of rotation of the moving octahedron pass through the origin and lie in a plane of reflection symmetry that passes through two vertices and cuts an edge at its midpoint (Fig.4a).



a. Axes of rotation



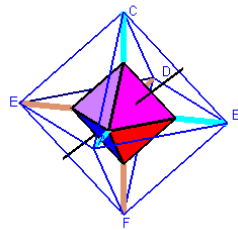
b. The quality index

Figure 4. The axes of rotation and the quality index

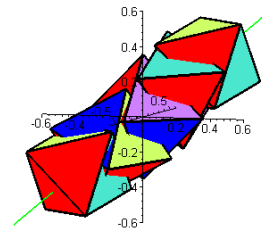
Fig.4a shows the axes of rotation for which the quality index is obtained and Fig.4b shows the quality index plotted as a function of ϕ and β . Here, ϕ denotes the angle of rotation about the axis and β is the angle between the axis of rotation and the Z-axis. The convention for measuring a positive sense of rotation is the usual one in which a positive angle advances a right hand screw along the positive direction of the screw axis. For this reason the rotation axes and screw axes are considered to be directed lines. The same notations and conventions will be used further in the paper. In Fig.4 the angle of rotation ϕ varies from $-\pi$ to $+\pi$, and the angle β is within the range $(0, \pi/2)$. The range of ϕ is shown in units of $\pi/15$, and the range of β is shown in units of $\pi/10$. The analysis was carried out for a variation of angle β throughout the full range $(0, 2\pi)$ but only the results for the range $(0, \pi/2)$ are shown in Fig.4. It is clear from Fig.4, that the quality index is zero for rotation of the moving octahedron about the axes of 2-fold and 4-fold rotation symmetry. This means that the robot is in singular configurations regardless of the angle of rotation about these axes. On the other hand, we determined that the robot reaches its best configuration (the quality index is 1 or -1) for a rotation about the axis of 3-fold rotation symmetry.

3.3 Axis of 3-Fold Rotation Symmetry

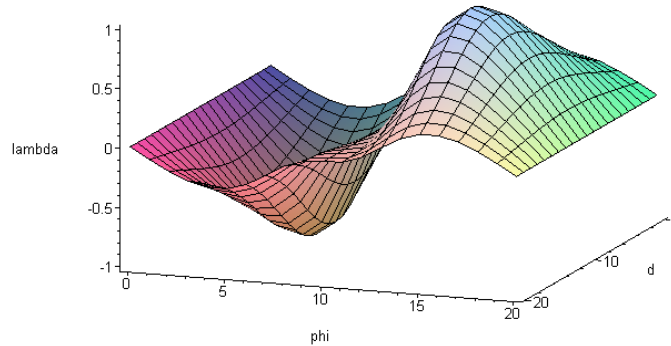
In this case, the quality index is obtained for translation and rotation along and about the axis of 3-fold rotation symmetry. The obtained quality index and the axis of 3-fold rotation symmetry for the octahedron are shown in Fig. 5.



a. The axis of 3-fold rotation symmetry



b. Some positions of the moving octahedron during the movement



c. The quality index

Figure 5. The axis of rotation, positions of the moving octahedron and the quality index

Here, the angle of rotation ϕ varies from $-\pi$ to $+\pi$, and the translation d varies from -0.5σ to $+0.5\sigma$ (in Fig. 5 the range of ϕ is shown in units of $\pi/10$, and the range of d is shown in units of 0.05σ). Obviously, the quality index is zero when the angle of rotation ϕ is $-\pi$, 0 , or $+\pi$, regardless of the translation. On the other hand, the quality index reaches its maximum (1 or -1) when the moving octahedron is in the center of the fixed one ($d = 0$) and rotates about the axis of 3-fold rotation symmetry.

4. Discussion and conclusions

The paper has examined some aspects of the behavior of (a new version of) the quality index for a 3D octahedral parallel manipulator system in terms of symmetry. The quality index has been plotted for two types of motion. The first involved the moving platform rotating about a sequence of axes lying in a plane of reflection symmetry. The second involved the moving platform screwing about an axis of 3-fold symmetry. Other types of motion have been explored but the details are not reported here.

Three main conclusions have resulted from this work. Firstly, the value of the quality index has been shown to be zero for all rotations about either an axis of 2-fold or an axis of 4-fold symmetry. (It is zero at the 'home' position of course, and it remains zero for any translation away from this position.) Secondly, the maximum value of the quality index occurs at each axis of 3-fold rotation symmetry for a particular angle of rotation. Finally, allowing the quality index to attain negative values leads to two separate types of configuration

- one for positive values and the other for negative values. Each of these two configurations has an extremum.

References

- Angeles, J., Lopez-Cajun, C. S. (1992), Kinematic isotropy and the conditioning index of serial robotic manipulators, *The International Journal of Robotics Research*, no. 6, vol. 11, pp.560-571.
- Duffy, J., Rooney, J., Knight, B. and Crane, C. D. (2000), A review of a family of self-deploying tensegrity structures with elastic ties, *The Shock and Vibration Digest*, no. 2, vol. 32, pp. 100-106.
- Lee, J., Duffy, J. and Hunt, K.H. (1998), A practical quality index on the octahedral manipulator, *The International Journal of Robotics Research*, no. 10, vol. 17, pp.1081-1090.
- Lee, J. Duffy, J. and Keler, M. (1999), The optimum quality index for the stability of in-parallel planar platform devices, *Journal of Mechanical Design*, vol. 121, pp.15-20.
- Lee, J., Duffy, J. and Rooney, J. (2000), An initial investigation into the geometrical meaning of the (pseudo-) inverses of the line matrices of the edges of platonic polyhedra, *Proceedings of a Symposium Commemorating the Legacy, Works, and Life of Sir Robert Stawel Ball Upon the 100th Anniversary of A Treatise on the Theory of Screws*, Trinity College, University of Cambridge, UK., July 9-12.
- Mayer St-Onge, B. and Gosselin, C. M. (2000), Singularity analysis and representation of the general Gough-Stewart platform, *The International Journal of Robotics Research*, no. 3, vol. 19, pp.271-288.
- Merlet, J-P. (1993), Direct kinematics of parallel manipulators, *IEEE Transaction on Robotics and Automation*, no. 6, vol. 9, pp.842-846.
- Rooney, J., Duffy, J. and Lee, J. (1999), Tensegrity and compegrity configurations in anti-prism manipulator platforms, *Proceedings of the Tenth World Congress on the Theory of Machines and Mechanisms*, Oulu, Finland, pp. 1278-1287.
- Stewart, D. (1965), A platform with six degrees of freedom, *Proceedings of Institution of Mechanical Engineers*, London, UK, no. 15, vol. 180, pp.371-386.
- Yoshikawa, T. (1985), Manipulability of robotic mechanism, *The International Journal of Robotics Research*, no. 2, vol. 4, pp.3-9.
- Zanganeh, K.E. and Angeles, J. (1997), Kinematic isotropy and optimum design of parallel manipulators, *The International Journal of Robotics Research*, no. 2, vol. 16, pp.185-197.